Environment, Development and Sustainability
https://doi.org/10.1007/s10668-026-07724-4

Life cycle climate impacts of lithium battery–powered refrigerated containers: comparative assessment and sensitivity analysis

Guanghai Liu[1] · Zongyu Chen[1] · Yuanxin He[2] · Hai Chang[2] · Junzhang Wu[3]

Received: 18 August 2025 / Accepted: 7 May 2026

Abstract

Decarbonizing temperature-controlled road freight is essential to sustainable food systems but complicated by the added energy demand of refrigeration. We perform a cradle-to-grave life cycle assessment (LCA) of 40—ft refrigerated containers comparing a diesel mechanical refrigerated container (MRC) with a battery-driven lithium refrigerated container (LRC). This study focuses on climate change impacts expressed as life cycle greenhouse gas (GHG) emissions (CO_2-equivalent). Under a China grid baseline, life-cycle GHG emissions are effectively equal: 60.97 vs 61.04 g $CO_2e/(t\cdot km)$ for MRC and LRC, respectively—a marginal + 0.12% for LRC. Operation dominates (~95% of life-cycle GHGs), led by traction energy. Although electrifying the refrigeration unit lowers use-phase emissions, gains are offset by (*i*) the mass penalty of the battery pack, which raises traction energy, and (*ii*) upstream emissions from battery manufacturing on a carbon-intensive grid. Sensitivity analyses show LRC becomes favorable with cleaner electricity, lower-emission battery production and recycling, low-GWP/low-leakage refrigerants, and reduced empty running. Conversely, when grid carbon intensity is high, electrifying refrigeration alone yields negligible benefit. Larger near-term mitigation likely comes from electrifying vehicle drive, power-system decarbonization, and logistics optimization. Additionally, although the LRC entails a modestly higher upfront investment, its lower operational energy demand translates into improved life-cycle economic performance. These results provide a transparent baseline for comparing lithium-battery and mechanical refrigeration pathways and clarify the grid, mass, and refrigerant conditions under which refrigeration electrification delivers measurable GHG reductions. The future research could extend this framework by incorporating non-CO_2 climate forcers, air pollutant emissions, and broader material-related environmental impacts to enable a more comprehensive sustainability assessment.

Graphical abstract

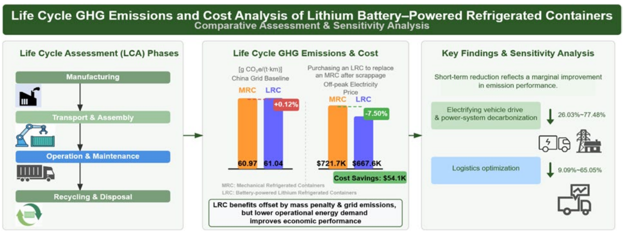

Extended author information available on the last page of the article

Published online: 12 May 2026

Keywords Transport · Refrigerated container · Lithium battery · Life cycle assessment · LCA · GHG emissions · Carbon footprint

1 Introduction

The transportation sector accounts for roughly one-quarter of global energy-related carbon dioxide (CO_2) emissions, making it a major contributor to overall greenhouse gas (GHG) emissions (Huo et al., 2024a; Zhang et al., 2024a,2024b). In China, 9% of total GHG emissions come from the transportation sector (Zhang et al., 2024a, 2024b). Within this sector, refrigerated transportation is especially energy-intensive because it must sustain continuous temperature control to preserve food freshness and safety (Dong et al., 2025; Kaptan & Bayazit, 2023). Its climate impact is further amplified by the relatively low operating energy efficiency of refrigeration units and the use of high Global Warming Potential (GWP) refrigerants (Han et al., 2024). Some assessments report that about 15% of global fossil-fuel energy is used for refrigerated food transportation and that ~ 40% of its GHG emissions arise directly from refrigeration equipment (Aliu et al., 2022). In China, high energy costs constrain cold-chain adoption: current refrigerated transport rates are only 15% for fruits and vegetables, 57% for meat, and 69% for aquatic products, and insufficient cold-chain operations are linked to annual food losses of about 70 billion yuan—roughly 20% of total production value (Liu et al., 2024). Against this backdrop, expanding cold-chain coverage while cutting GHG emissions necessitates replacing diesel-based systems with lower-carbon energy carriers and refrigerants, laying the groundwork for the pathway analyses in this study.

Electrification is widely promoted as a cornerstone of transport decarbonization, and adoption is accelerating—China's market share of electric vehicles (EVs) reached over 60% globally in 2023, and it is expected to continue to grow (Zhang et al., 2025). Beyond zero tailpipe emissions, EVs offer higher drivetrain efficiency and rapidly improving battery technology (energy density, safety, cost) (Moreno Sader et al., 2025). Empirical estimates of the mitigation benefit, however, span a wide range because system boundaries and operating contexts differ. For light-duty use under relatively clean grids, studies report sizable reductions: EVs could cut GHGs by ~ 47% in Guo et al. study and ~ 22.6% in Farzaneh and Jung study, respectively (Farzaneh & Jung, 2023;Guo et al., 2023a). Yet under carbon-intensive power, electrification can underperform: Moreno Sader et al. found electric trucks emitting roughly twice those of diesel due to high grid intensity, and a global-mix case for a Volvo model shows only a 6.90% reduction potential (Moreno Sader et al., 2025; Volvo Cars, 2022). These discrepancies are systematic rather than contradictory. They arise from (*i*) scope choices (tank-to-wheel vs well-to-wheel vs cradle-to-grave, inclusion of battery manufacturing and end-of-life), (*ii*) electricity assumptions (average vs marginal grid intensity, charging time/location, renewable matching), and (*iii*) duty-cycle realities (vehicle class, speed/load profiles, ambient temperature). For refrigerated transport specifically, auxiliary cooling loads and battery mass can erode efficiency gains, while depot charging with low-carbon electricity can amplify them. The implication is clear: electrification delivers robust emissions cuts when paired with cleaner power and use-case-appropriate design/operation; without grid decarbonization and smart charging, benefits shrink and can invert—especially for heavy, refrigeration-equipped duty cycles.

Building on passenger-car electrification, technology and supply-chain spillovers are accelerating the shift to electric transport refrigeration. In China, electric refrigerated trucks now hold 8.76% market share, and Original Equipment Manufacturers (OEMs) are commercializing electric Transport Refrigeration Units (TRUs), e.g., Carrier's unit is estimated to cut annual operating expenditure by ~ 2,300 CNY (Chinese association of refrigeration, 2025). At the container scale, lithium-battery systems report up to 89.17% operating-cost savings (He et al. 2024). Yet most evaluations emphasize use-phase energy while overlooking cradle-to-grave burdens—battery and power-electronics manufacturing, additional vehicle mass, refrigerant choice and leakage, maintenance, and end-of-life—risking burden shifting across life-cycle stages. Given China's high-carbon grid, upstream electricity and battery production can also erode or reverse operational gains. These uncertainties motivate a full Life Cycle Assessment (LCA) that moves beyond the refrigeration subsystem to the vehicle–container system and tests sensitivity to grid carbon intensity, battery sizing, and refrigerant GWP to determine whether electrified refrigeration delivers net emission reductions in the near term.

To bridge the gap between promising trial-phase savings and system-wide climate outcomes, we conduct a cradle-to-grave LCA of 40—ft Mechanical Refrigerated Containers (MRCs) versus battery-powered Lithium Refrigerated Containers (LRCs). The model spans raw-material extraction and manufacturing (battery/engine, compressor, box and insulation), assembly and distribution, the use phase (traction and refrigeration energy under an identical duty cycle, refrigerant charge/leakage, maintenance), and end-of-life (recycling/disposal), with a harmonized functional unit (per t·km of cooled freight at a fixed set-point) and region-specific energy carbon intensities. We compare total GHG emissions and decompose stage contributions, then run sensitivity tests for key levers—including grid carbon intensity and charging mix, battery mass and cycle life, refrigerant type/leakage, ambient temperature and heat load, and empty-running/vehicle utilization—to pinpoint when and why battery-powered LRCs deliver net reductions. The results inform targeted promotion strategies (e.g., cleaner charging, low-GWP refrigerants, weight/route optimization) to unlock robust emission cuts beyond operational cost savings.

2 Materials and methods

2.1 Goal and scope definition

2.1.1 The goal of study

This study develops a life cycle GHG emission model for the diesel-driven MRC and the proposed battery-powered LRC using the LCA method following ISO 14044 and ISO 14067 standards (ISO 14044, 2006; ISO 14067,2018). By comparing the environmental impacts of the two systems, this study highlights critical emission differences, and proposes targeted strategies to promote the sustainable development of next-generation refrigerated transport technologies. Consistent with ISO 14067, this study is explicitly designed as a carbon footprint assessment focusing on climate-change impacts expressed in CO_2-equivalents. Accordingly, non-CO_2 climate forcers (e.g., black carbon) and other environmental impact categories, such as air pollutant emissions (e.g., NO_x, SO_2, particulate matter), photochemical ozone formation, and ozone depletion, are excluded from this assessment.

This study examines two 40-foot refrigerated containers manufactured by CRRC Corporation Limited (https://www.crrcgc.cc/en/), the second-largest producer of refrigerated c ontainers in China. Technical specifications for both containers were obtained directly from CRRC. The two container types, i.e., MRC (Fig. 1a) and battery-powered LRC (Fig. 1b), use the same refrigerant, R404A, with a charge amount of 6 kg. However, they are equipped with different refrigeration systems: the MRC utilizes the SLXe-400 unit, while the battery-powered LRC is fitted with the CRRC-KX1200EW unit. The MRC's refrigeration unit is powered by a diesel engine, whereas the LRC's unit is driven by a lithium battery (see Fig. 1c). In the LRC system, refrigeration is powered by electricity supplied by onboard lithium battery energy storage, decoupling cooling demand from diesel combustion during operation. Despite these differences, both container types rely primarily on diesel fuel for transportation. This study assumes that heavy-duty refrigerated transport equipment is diesel-powered, with pure lithium—battery—driven solutions not being considered. The primary reason is that under the current technological conditions, electric heavy—duty trucks still face significant constraints in long—distance heavy—load transportation. Restricted by the energy density of lithium batteries, to achieve a driving range of hundreds of kilometers, large—capacity batteries need to be configured. The weight of these batteries will significantly occupy the legal cargo—carrying mass and impair the transportation economy. Meanwhile, the purchase cost of the entire vehicle equipped with power batteries is significantly higher than that of diesel vehicles of the same class. In addition, the charging time and infrastructure requirements brought about by large—capacity batteries are difficult to meet the demands of high—frequency continuous operation. Overall, under the current conditions of load capacity, driving range, cost and energy—supplementing conditions, lithium—battery—driven solutions are still difficult to meet the actual operational needs of heavy—duty refrigerated transportation. Therefore, diesel power is adopted as the benchmark assumption in this paper.

2.1.2 Functional unit

The functional unit (FU) of this study is defined as grams of CO_2-equivalent emissions per tonne-kilometer of goods transported, expressed as g CO_2eq/(t·km). This unit is widely adopted in environmental assessments of freight transport systems and is consistent with the Product Environmental Footprint Category Rules (PEFCR) guidance for transport-related products, as well as ISO 14044 and ISO 14067 standards. The selection of this turnover-based functional unit ensures a comparative basis between different refrigerated container systems—specifically the conventional MRC and the proposed battery-powered LRC. It reflects the environmental burden per unit mass of cargo moved over a unit distance, thereby capturing the combined influence of emissions from energy consumption, refrigeration efficiency, and logistics performance across the full life cycle.

2.1.3 System boundary

This study adopts a cradle-to-grave system boundary for both the MRC and the battery-powered LRC, encompassing all relevant life cycle stages as illustrated in Fig. 2. The analy-

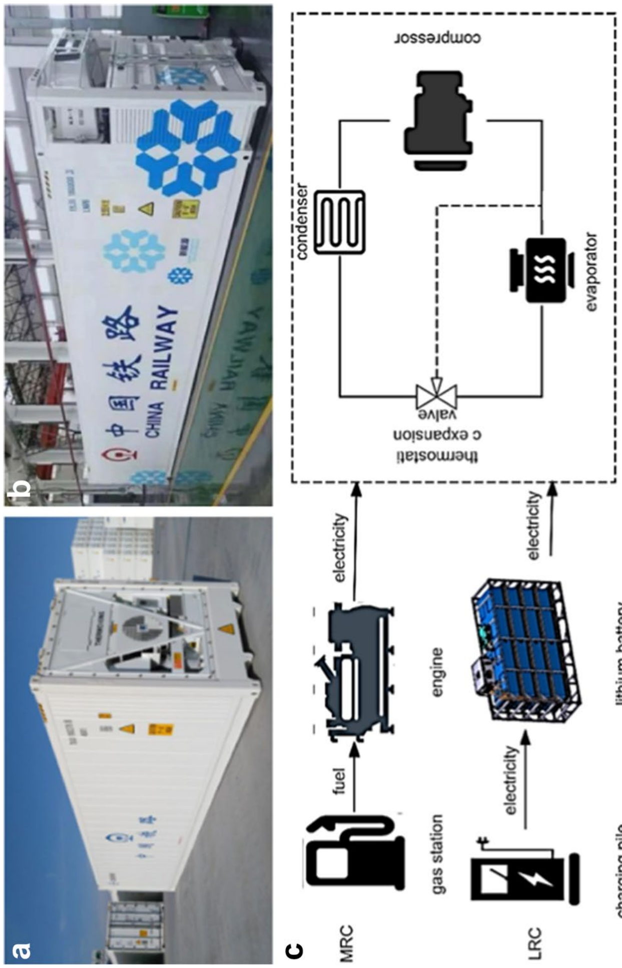

Fig. 1 Physical diagrams and mechanisms: (**a**) conventional mechanical refrigerated container (MRC); (**b**) battery-powered lithium refrigerated container (LRC); and (**c**) schematic illustration of the operating principles of MRC and LRC systems

sis is structured into four main phases: production, transport and assembly, operation and maintenance, and end-of-life recycling. In the production stage, the system includes the extraction and processing of raw materials, as well as the manufacturing and assembly of key components such as the enclosure structure, refrigeration unit, and the power system, represented by a diesel engine in the case of MRC and a lithium-ion battery in the case of LRC. The use of refrigerant (R404A) is also accounted for, including its production and initial charging. The transport and assembly stage includes emissions arising from the logistics of delivering components to the assembly site, on-site integration of refrigeration and power systems, and the deployment of the final container to its operational location. This stage also considers potential refrigerant leakage during initial installation. The operation and maintenance stage captures the energy consumed during the use phase, including diesel combustion for MRC and electricity usage for LRC battery charging, as well as regular maintenance activities and fugitive emissions due to refrigerant leakage over time. Finally, the recycling stage accounts for the disassembly, material recovery, and final disposal of container components, incorporating emissions from energy used in dismantling and transport, avoided burdens from material recycling, and residual emissions from landfilling or incineration. Infrastructure related to roads, ports, and warehouses, as well as human-related activities, are excluded from the system boundary. To focus on climate change impacts reflected by life-cycle GHG emissions expressed as CO_2-equivalents, material-related impacts beyond GHG emissions, such as resource depletion and toxicity associated with battery materials, are not assessed and therefore fall outside the scope of this carbon footprint–oriented study. A 20-year service life is assumed for both container types to ensure comparability, and functional equivalence in cooling performance, payload, and transport characteristics is maintained throughout the analysis (Fig. 2).

2.1.4 Data source and quality

The life cycle inventory (LCI) data used in this study was obtained from a combination of peer-reviewed scientific literature, direct communication with relevant enterprises, and publicly available databases provided by national regulations, industry standards, and technical guidelines. These sources collectively ensure transparency, credibility, and representativeness of the data applied in modeling the environmental performance of the MRC and the battery-powered LRC. For both systems, we conducted a comprehensive review and critical evaluation of the available information to extract key inventory parameters, including material composition, energy and fuel consumption, refrigerant use and leakage rates, transportation logistics, and end-of-life treatment processes. Special attention was given to capturing the specific characteristics of each container type—such as the lithium-ion battery system in the LRC and the diesel engine in the MRC—to reflect technological differences in inventory modeling. The compiled data were then used to construct complete LCIs for both MRC and battery-powered LRC across all stages: production, transport and assembly, operation and maintenance, and recycling. Wherever possible, region-specific and technology-specific data were applied to enhance the geographical and temporal relevance of the assessment. Data set developed for each supply chain stage is presented in Sect. 2.2. Data analysis was performed using Microsoft Excel 2021, and data visualization was conducted using OriginPro 2025b.

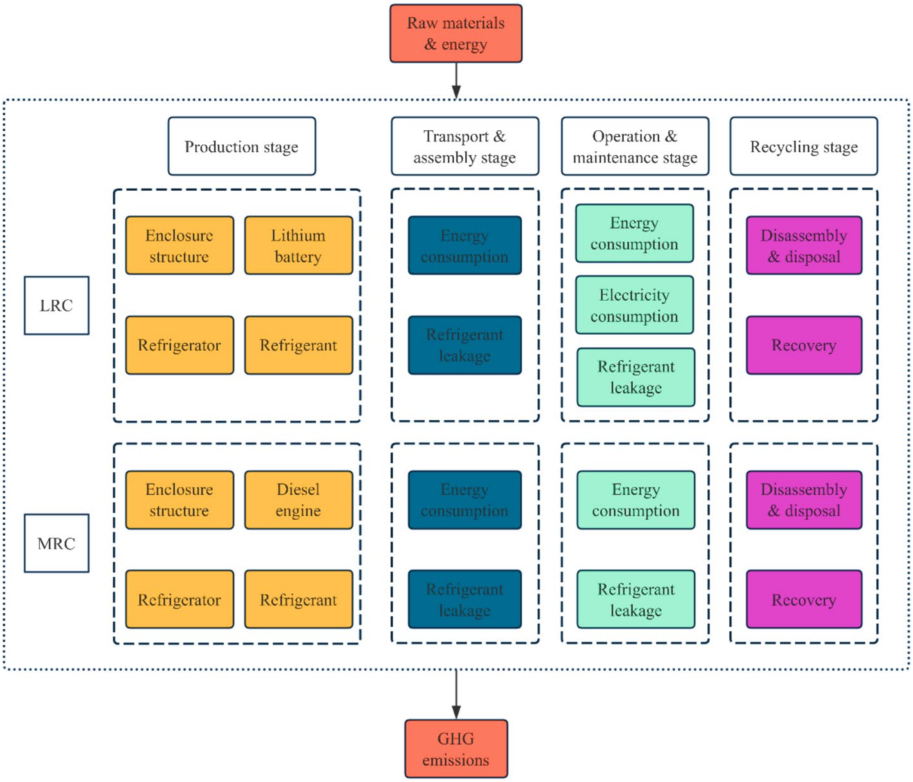

Fig. 2 System boundaries of the MRC and battery-powered LRC, covering production, transport and assembly, operation and maintenance, and recycling stages, including key sources of GHG emissions

2.2 Life cycle inventory analysis

The LCA model considers environmental impacts across the material production, transportation and assembly, operation and maintenance and recycling stages, aggregating them to estimate the overall GHG emission of the specific transport refrigeration unit. The formula for calculating GHG emissions throughout the entire life cycle of refrigerated containers is consistent for mechanical and lithium battery refrigerated containers. The primary difference is that mechanical and lithium battery refrigerated containers use different energy methods to drive the refrigeration units, diesel and electricity respectively. The total GHG emissions (C) for the entire life cycle are calculated using Eq. (1) based on actual conditions. The detailed emission factor for each stage is summarized in Supporting Information.

$$C = C_P + C_{TA} + C_{OM} + C_R \tag{1}$$

2.2.1 Production stage

During the production stage, GHG emissions arise primarily from energy and material inputs. These inputs are required to manufacture the container's key components, including the enclosure structure, the power unit (i.e., diesel engine for MRC or lithium-ion battery for LRC), and the refrigeration system (comprising both the mechanical unit and refrigerant). Production-stage emissions (C_P) are quantified using Eq. (2) and represent the embodied GHG emissions of these materials and subsystems prior to assembly.

$$C_P = \sum m_i \times \beta_{P-i} \tag{2}$$

where m_i is the weight of material i, in kg; C_{P-i} is the GHG emissions factor of material i in kg CO_2eq/kg.

Specifically, the carbon footprint of the refrigeration unit and refrigerant during the production process is 17.27 kg CO_2eq/kg and 30.00 kg CO_2eq/kg, respectively, as reported in Wu et al., (2022a, 2022b). For the battery-based LRC system, the power unit consists of a lithium iron phosphate (LFP) battery with a rated capacity of 282 kWh. The production-related carbon intensity for LFP batteries is estimated at 95.1 kg CO_2eq/kWh, based on Feng et al. (2022), resulting in a total battery-related emission of approximately 26,816 kg CO_2eq. For the container's enclosure structure, the production emission is calculated based on the total weight of component materials (e.g., steel, insulation foam, and aluminum) and their respective emission factors, resulting in an average production carbon intensity of 3.42 kg CO_2eq/kg, as reported by Wang et al. (2025). All input data and emission factors applied in the production stage are summarized in Table 1, which forms the basis for the inventory modeling of this stage.

2.2.2 Transport and assembly stage

The transportation of equipment components is a critical part of the refrigerated container assembly process, involving the movement of major subsystems—such as the enclosure structure, refrigeration unit, diesel engine, or lithium battery—from the manufacturing site to the final assembly center. This stage results in GHG emissions primarily due to fuel consumption by transport vehicles. The unit fuel consumption for component transportation is estimated at 4.45×10^{-5} L/(kg.km), as reported in Wu et al. (2022a), and forms the basis for calculating energy-related emissions in this phase. In addition to fuel-related emissions, direct GHG emissions from refrigerant leakage during the installation of refrigeration systems are also considered. Based on Fabris et al. (2024), a leakage rate of 2% of the total refrigerant charge is applied to reflect installation-stage losses. The total GHG emissions for the transport and assembly stage, denoted as C_{TA}, are calculated using Eq. (3), which integrates both fuel-based emissions and refrigerant-related impacts.

Table 1 LCI data for the production stage

Component	Weight/Capacity	Emission factor	Source
Enclosure structure	1687.8 kg	3.42 kg CO_2eq/kg	(Wang et al., 2025)
Refrigerator	380 kg	17.27 kg CO_2eq/kg	(Wu et al. 2022)
Refrigerant	6 kg (R404A)	30 kg CO_2eq/kg	(Wu et al. 2022)
Lithium battery	1800 kg (282 kWh)	95.1 kg CO_2eq/kWh	(Feng et al., 2022)

$$C_{TA} = \sum m_j \times D_j \times f + L_{TA} \times GWP \tag{3}$$

where m_j represents the weight of component j, in kg; D_j represents the distance from the assembly line to the assembly center, in km; f denotes the GHG emissions factor of the vehicle, in kg CO_2eq/(kg.km); L_{TA} is the refrigerant leakage during the transportation and assembly stage, in kg; GWP is the global warming potential of refrigerant.

2.2.3 Operation and maintenance stage

During the operation and maintenance stage, GHG emissions arise from both indirect energy consumption and direct refrigerant leakage. Indirect emissions result from the use of energy by the traction device (i.e., truck or transport vehicle) and the refrigeration unit, while direct emissions are attributed to the leakage of refrigerants during operation—often caused by vibrations, temperature fluctuations, and mechanical wear during long-distance transportation. The total GHG emissions associated with this stage, denoted as C_{OM}, are calculated using Eqs. (4) to (6).

$$C_{OM} = E_1 \times \beta_E + E_2 \times \beta_f + L_{OM} \times GWP \tag{4}$$

$$E_1 = EC_R \div COP \div \theta \times N \times Y \times (1 - R_{EL}) \times 24 \tag{5}$$

$$E_2 = FC_1 \times D \times (1 - R_{EL}) \times N \times Y + FC_2 \times D \times R_{EL} \times N \times Y \tag{6}$$

where E_1 represents the refrigeration energy consumption over the entire life cycle, in kWh; β_E represents the emission factor of the energy used by the diesel engine or lithium battery, in kg CO_2eq/kWh; E_2 represents the total energy consumption required for driving over the entire life cycle, in kWh; EC_R represents the refrigeration capacity of the refrigeration unit, in kW; L_{OM} represents the leakage of refrigerant during operation, in kg; N represents the number of transport trips in a year; Y represents the service life of the equipment; R_{EL} represents the empty-loaded rate; FC_1 represents the fuel consumption when fully loaded, in L/km; FC_2 represents the fuel consumption when empty, in L/km; D represents the transportation distance per trip of the equipment, in km; β_f represents the emission factor of diesel, in kg CO_2eq/kWh.

In this study, it is assumed that diesel fuel is used to power the traction devices of both container types. For refrigeration, MRC systems consume diesel fuel, whereas battery-based LRC systems utilize electricity stored in lithium battery packs. Refrigerated containers are primarily employed for transporting frozen products, with the internal temperature maintained at –18 °C. Under these conditions, the coefficient of performance (COP) of the refrigeration system is assumed to be 0.8, based on Wu et al. (2022a). In terms of refrigerant emissions, it is estimated that 25% of the refrigerant charge leaks annually during the operational phase, consistent with real-world cold chain operation data reported by Wu et al. (2022a).. The refrigerant used in both systems is R404A, which has a GWP of 4,728 over a 100-year time horizon, according to the Intergovernmental Panel on Climate Change (IPCC) Sixth Assessment Report (AR6). The emission factors applied in this stage are 2.58 kg CO_2eq/L for diesel fuel and 0.56 kg CO_2eq/kWh for electricity, based on data from Cui et al. (2025) and Ritchie et al. (2020), respectively. All input data relevant to this stage, including emission factors, energy use assumptions, and refrigerant leakage rates, are summarized in Table 2.

Table 2 The LCI data during the operation and maintenance stage

Variable	Quantity	Source
Annual leakage rate of refrigerant	25%	(Wu, et al. 2022)
The emission factor of diesel (kg CO_2eq/L)	2.58	(Cui et al., 2025)
The emission factor of electricity (kg CO_2eq/kWh)	0.56	(Ritchie et. al 2020)
Full-loaded fuel consumption (L/100 km)	35	Survey data
Empty-loaded fuel consumption (L/100 km)	28	Survey data
Empty-loaded rate	50%	Survey data

2.2.4 Recycling stage

The standard operational lifespan of a refrigerated container is assumed to be 20 years, after which the unit is decommissioned. The end-of-life stage involves a combination of recycling and disposal processes targeting the enclosure structure, power system (diesel engine or lithium battery), refrigeration unit, and refrigerant. This stage is crucial for minimizing both environmental impacts and resource loss, and its associated GHG emissions are denoted as C_R, calculated using Eq. (7).

$$C_R = \sum m_i \times \theta_i \times \beta_{R-i} \tag{7}$$

where θ_i is the material i recovery rate; β_{R-i} denotes the recycling GHG emission factor for material i, in kg CO2eq/kg.

During decommissioning, the refrigeration unit and remaining refrigerant are partially recovered. The carbon footprint associated with the recovery and treatment of refrigeration units and refrigerants is estimated at 6.6 kg CO_2eq/kg and 305.6 kg CO_2eq/kg, respectively, based on Wu et al. (2022a). It is assumed that only 10% of the refrigerant is successfully recovered, while the remaining 90% is emitted directly into the atmosphere, contributing to substantial climate impact due to the high GWP of R404A. For the battery-powered LRC system, the recycling of LFP batteries is also considered. The carbon emission intensity for LFP battery recycling is estimated at 2.9 kg CO_2eq/kWh, based on (Tao et al., 2023). The recovery and treatment of the enclosure structure are modeled using an average emission intensity of 1.83 kg CO_2eq/kg, as reported by Wang et al. (2025). These assumptions and emission factors form the basis for calculating end-of-life impacts and are incorporated into the overall life cycle model to ensure a complete cradle-to-grave assessment.

2.3 Life cycle cost assessment

When conducting a life-cycle cost analysis, enterprises must take into account the total cost of refrigerated containers from their initial purchase to final disposal (Hao et al., 2024; Li et al., 2024). This includes the initial purchase cost, operating cost, and final disposal cost of both types of containers (see Eq. 8). The initial purchase cost is provided by the equipment manufacturer, with MRC and battery-based LRC being $34,000 and $45,000 respectively. According to China's current purchase subsidy policies for new EVs, the acquisition cost of the battery-based LRC can be substantially reduced through policy incentives: under the vehicle scrappage-and-replacement subsidy scheme, the purchase cost can be lowered from $45,000 to approximately $25,000, while under the early scrappage subsidy scheme, the cost can be reduced to around $40,000, thereby significantly enhancing its economic viability and market competitiveness. The final disposal cost is uniformly assumed to be 10% of the initial purchase cost to reflect the costs related to equipment retirement, dismantling, and residual value processing. The operating cost mainly consists of energy consumption cost and maintenance cost, with the maintenance cost calculated using the proportion method. Considering the complex structure, numerous components, and high requirements for lubrication and regular maintenance of diesel engine systems, the maintenance cost of MRC is set at 15% of its initial purchase cost; in contrast, the mechanical structure of battery-based LRC driven by lithium batteries is relatively simplified and has a lower maintenance frequency, with its maintenance cost assumed to be 7.5% of the initial purchase cost. This differentiated setting is consistent with the conclusion in existing studies that there is a significant difference in maintenance costs between fuel-powered transportation equipment and electric transportation equipment (Guo et al., 2023b; Qiao et al., 2020). This analysis ensures that companies have a comprehensive understanding of the financial implications of refrigerated container ownership, from the outset through to the end of its lifecycle.

$$Q = Q_1 + Q_2 + Q_3 \tag{8}$$

$$Q_2 = \sum E \times P_E + Q_M \tag{9}$$

where Q is the life-cycle cost, in dollars; Q_1 is the acquisition cost, in dollars; Q_2 is the operation and maintenance cost, in dollars; Q_3 is the disposal cost, in dollars; E is the total amount of energy required for a refrigerated container over its entire life cycle, in kWh; P_E is the price of the energy, in dollars/kWh; Q_M is the maintenance cost, in dollars.

3 Results and discussion

3.1 Life cycle GHG emission assessment

Figure 3 compares the life cycle GHG emissions of the diesel-based MRC and the battery-powered LRC across four stages. The total GHG emissions amount to 60.97 g CO_2eq for the MRC and 61.04 g CO_2eq for the battery-based LRC per functional unit, corresponding to a marginal increase of 0.12% for the battery-powered system. This negligible difference reveals a critical trade-off in the current system configuration: while the battery-based LRC achieves lower operational emissions through electrified refrigeration, this advantage is significantly offset by its higher transport-related emissions. The key driver of this trade-off is the weight disparity between the two systems. The lithium battery pack of the LRC weighs approximately 1,800 kg, compared with 772 kg for the diesel engine used in the MRC, resulting in a total unit weight of 3.91 t for the battery-based LRC versus 2.88 t for the MRC. As transport-stage emissions scale with payload mass under diesel-based trucking assumptions, the additional battery weight increases fuel consumption and associated GHG emissions, particularly in long-haul operations (Moreno Sader et al., 2025). This finding

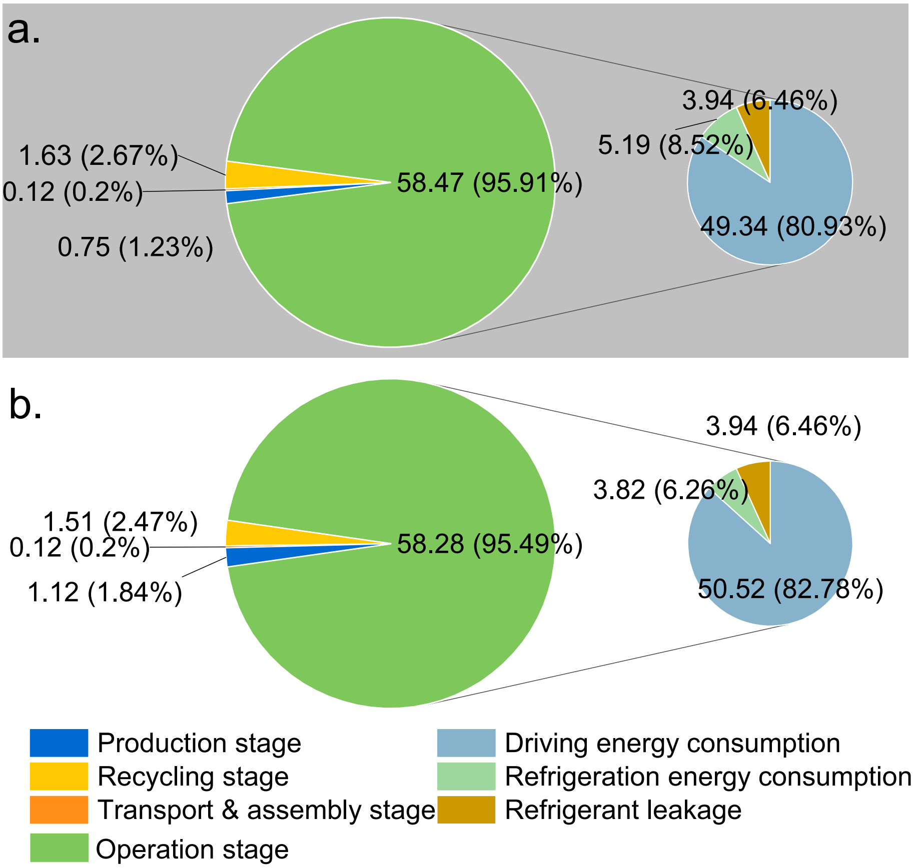

Fig. 3 The GHG emissions distribution for the diesel-based MRC (**a**) and battery-powered LRC (**b**) across their life cycle. The large circles represent total GHG emissions, while the zoomed-in smaller circles highlight contributions from the operation & maintenance stage. Values are shown in g CO_2eq/(t.km) and percentage share of total emissions

highlights the sensitivity of climate performance to system design choices under current freight transport conditions.

The operation and maintenance stage is the predominant contributor to total emissions in both systems, accounting for 95.91% of emissions in MRC (58,47 g CO_2eq) and 95.49% in battery-powered LRC (58,28 g CO_2eq). This small difference is largely due to the energy source and conversion efficiency. The diesel-based MRC relies on diesel combustion via a relatively inefficient engine to power its refrigeration system, resulting in high fuel-related emissions (Volvo Cars , 2023). In contrast, battery-powered LRC employs battery-electric refrigeration powered by onboard lithium iron phosphate (LFP) batteries, enabling higher energy conversion efficiency and reduced reliance on diesel fuel during operation (Moreno Sader et al., 2025). This electrification of the refrigeration function constitutes the main source of operational GHG mitigation in the battery-based LRC system.

However, this operational advantage is partly counterbalanced by higher emissions in the production stage for the battery-powered LRC (1.12 g CO_2eq) compared with the diesel-based MRC (0.75 g CO_2eq). This increase is driven by the material- and energy-intensive manufacturing of LFP batteries, which require substantial inputs of metals and electricity (Guo et al., 2023a, 2023b). As the present assessment focuses on climate-change impacts expressed as CO_2-equivalent emissions, material-related environmental impacts beyond GHG emissions (e.g., resource depletion or toxicity) are not explicitly addressed. Moreover, the magnitude of production-stage emissions is highly dependent on the electricity mix used in battery manufacturing, underscoring the importance of low-carbon power systems in maximizing the climate benefits of battery-based technologies (Feng et al., 2025).

At the end-of-life stage, the battery-powered LRC exhibits greater potential for GHG mitigation through improved recycling of battery materials. Advanced recycling pathways can recover valuable materials and offset upstream emissions, thereby enhancing the net climate performance of the LRC over its full life cycle. Overall, these results identify the operation stage as the dominant environmental hotspot while emphasizing that future improvements in battery energy density, manufacturing decarbonization, freight electrification, and recycling efficiency will be critical to unlocking the full climate mitigation potential of battery-powered refrigerated containers (Jiang et al., 2025; Moreno Sader et al., 2025; Quan et al., 2025; Wan et al., 2025).

3.2 Sensitivity analysis

To better understand the influence of key parameters and technological assumptions on the life cycle GHG emissions of battery-powered LRC, a sensitivity analysis was conducted following LCA best practices. This analysis focuses on three critical stages identified as environmental hotspots or intervention points in the baseline scenario: (1) LFP battery production, (2) operational electricity use, and (3) end-of-life recycling technologies. Specifically, for the production stage, we modeled changes in GHG emissions associated with LFP battery manufacturing, with an emphasis on variations in the carbon intensity of raw material supply and energy input. For the operation stage, we compared the GHG emissions of LRC under different national electricity grid mixes, reflecting country-specific fossil fuel shares and renewable energy integration in 2024. Finally, for the recycling stage, we evaluated three mainstream LFP recycling pathways—hydrometallurgical recycling, physical recycling, and cascade utilization—to examine their potential to reduce end-of-life carbon emissions.These scenario-based simulations allow us to quantify the sensitivity of LRC's environmental performance to improvements in upstream production efficiency, regional electricity decarbonization, and end-of-life circularity. Results are presented in Fig. 4, with all values expressed in g CO_2eq/(t·km) to ensure consistency with the functional unit defined earlier.

As illustrated in Fig. 4a and b, reductions in the carbon intensity of LFP production—either through cleaner electricity or more efficient raw material use—have a measurable impact on the production-stage emissions of LRC. When the carbon intensity of LFP manufacturing is reduced by 20% (from 100 to 80%), the GHG emissions in the production stage decline from 1.12 to 0.97 g CO_2eq/(t·km), representing a 13.3% reduction. However, this translates into only a marginal 0.24% decrease in total life cycle GHG emissions (from 61.04 to 60.89 g CO_2eq/(t·km)). This asymmetry underscores the fact that while LFP manufacturing is carbon intensive, the operation stage remains the dominant hotspot, limiting the influence of upstream optimization on overall system performance. It also reflects the structural challenges under China's fossil-fuel-heavy electricity grid, where both battery produc-

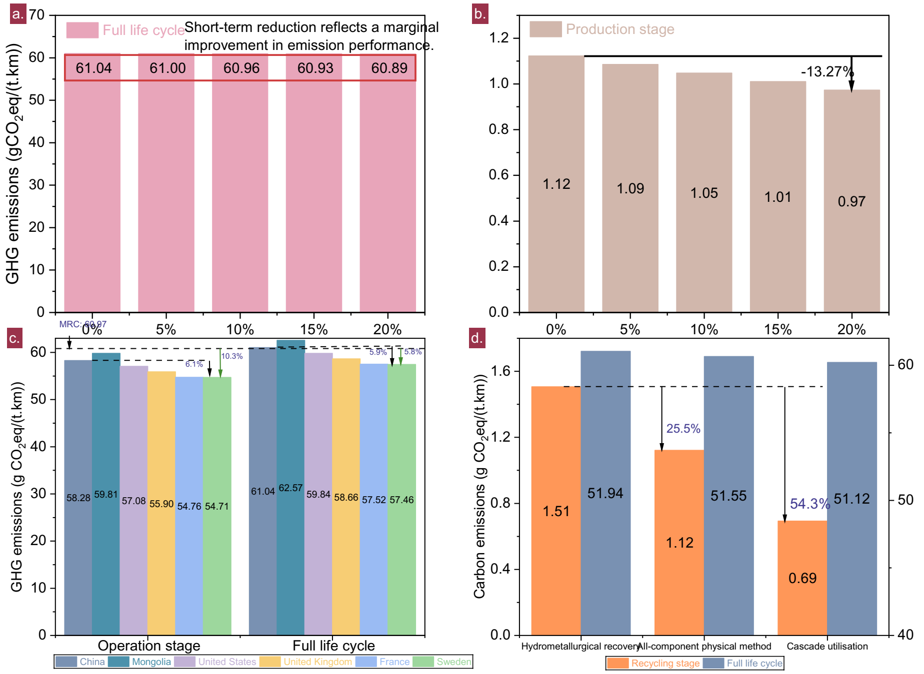

Fig. 4 Sensitivity analysis of the life cycle GHG emissions of battery-powered LRC under different scenarios: **(a)** Full life cycle GHG emissions of battery-powered LRC under varying carbon emission intensities of LRC battery production; **(b)** Emissions of battery-powered LRC in the production stage only, under different LRC production emission intensities; **(c)** Emissions of battery-powered LRC in the operation stage (left) and full life cycle (right) under different national electricity mixes (China, Mongolia, United States, United Kingdom, France, and Sweden); **(d)** Emissions of battery-powered LRC in the recycling stage and corresponding total emissions, under different LRC battery recycling technologies

tion and operational electricity use are indirectly affected by high grid carbon intensity. Given that raw material extraction contributes around 40% of total LFP production emissions (Manjong et al., 2024), further reductions in the production footprint would require simultaneous decarbonization of both electricity inputs and material supply chains. In contrast, Fig. 4c shows that changes in the carbon intensity of electricity used during operation have a more pronounced effect on the battery-based LRC's overall GHG emissions. The modeled scenarios indicate that countries with cleaner electricity grids, such as France (nuclear-dominated) and Sweden (renewables-dominated), offer significantly better environmental outcomes. Compared with China's baseline scenario, switching to the electricity structure of France or Sweden reduces the operational emissions of LRC by 6.0%—6.1%. At the full life cycle level, this translates to around 5.8% lower total emissions compared to MRC. However, in carbon-intensive regions such as Mongolia, where the electricity mix is predominantly coal-based, the battery-based LRC emissions during operation can exceed those of MRC—by as much as 2.6%—demonstrating that electrification alone is not a guarantee of climate benefit unless supported by low-carbon power sources. Figure 4d explores the sensitivity of end-of-life emissions to different battery recycling technologies. Among the three methods analyzed—hydrometallurgical recycling, physical recycling, and cascade utilisation—the latter proves to be the most environmentally beneficial, reducing recycling-stage emissions from 1.51 to 0.69 g CO_2eq/(t·km), a 54.0% reduction. Physical recycling achieves a moderate footprint of 1.12 g CO_2eq/(t·km), equating to a 25.5% reduction compared to hydrometallurgy. However, the technical feasibility of cascade use is currently constrained by battery quality requirements and market demand for secondary applications, while physical recycling faces challenges related to electricity consumption, equipment cost, and system complexity.

Together, these findings emphasize a system-level understanding of climate mitigation strategies for refrigerated container technologies. While upstream improvements in battery production and downstream recycling can contribute to emissions reduction, their impacts are often constrained or diluted without broader structural changes—particularly in the electricity mix during the operation phase. Therefore, to unlock the full potential of battery-based LRC in decarbonizing cold chain logistics, a coordinated approach is required, one that combines clean energy transition, green material sourcing, and efficient circular end-of-life management. Furthermore, this analysis highlights the importance of regionalized LCA modeling, as identical technologies can yield divergent environmental outcomes across different national contexts.

3.3 Evaluation of emission reduction measures

Figure 5 compares the life cycle GHG emissions of refrigerated container under two electrification pathways, i.e., grid-powered electric drive and battery-powered LRC, across multiple national contexts. Each pair of bars corresponds to a country's electricity structure in

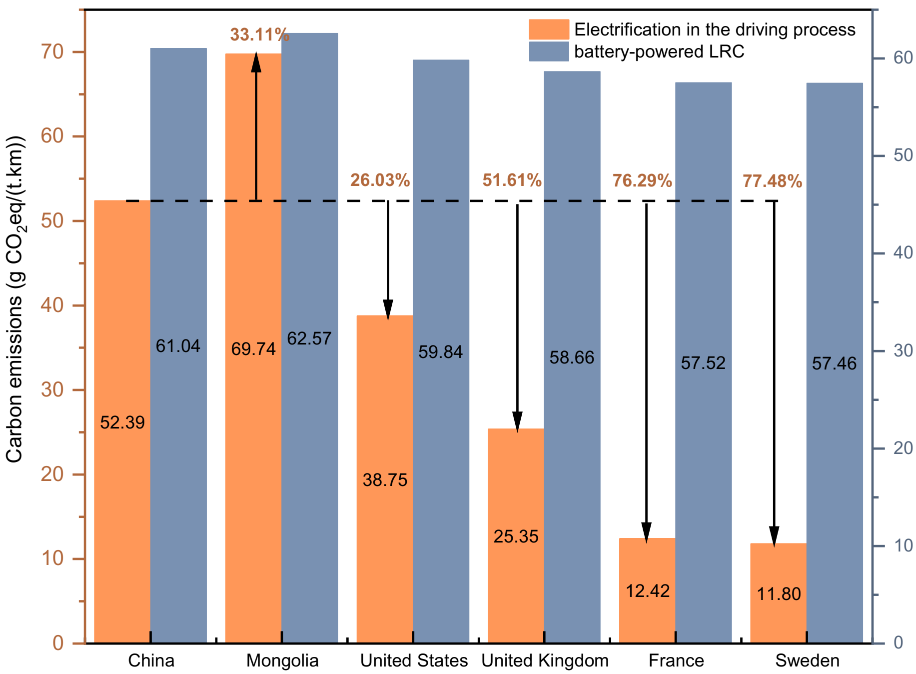

Fig. 5 Life cycle GHG emissions of refrigerated transport under grid-electric (left) and lithium battery-electric (right) drive across six countries

2024, reflecting the climate impact of deploying either grid-based electric trucks or battery-electric trucks within that local energy mix. The results show that in countries with high shares of fossil fuels in their electricity generation (e.g., Mongolia, China, United States), grid-powered electric vehicles generate substantially higher emissions than LRC-driven alternatives. For example, in Mongolia, the grid-electric vehicle emits 69.74 g CO_2eq, while the battery-powered LRC emits 60.51 g CO_2eq, resulting in a 13.2% reduction. In China, emissions from grid-electric vehicles are 61.04 g CO_2eq, compared to 52.39 g CO_2eq for the battery-powered LRC, yielding a 14.1% reduction. In the United States, the advantage of the battery-powered LRC is even more pronounced: emissions fall from 59.84 to 38.75 g CO_2eq, a 35.2% reduction. Countries with cleaner electricity mixes, such as France (high nuclear) and Sweden (high renewables), show dramatic reductions in carbon emissions from using battery-powered LRC. In France, the battery-powered LRC results in emissions of 12.42 g CO_2eq, compared to 57.52 g CO_2eq for the grid-electric case—a 78.4% reduction. Similarly, in Sweden, emissions fall from 57.46 to 11.80 g CO_2eq, equivalent to a 79.5% reduction. In the United Kingdom, the difference is also notable, with battery-powered LRC systems emitting 25.35 g CO_2eq, compared to 58.66 g CO_2eq for grid-electric—a 56.8% drop.

These findings suggest that the cleaner the grid, the more effective the battery-powered LRC system becomes, especially since battery charging can be decoupled from real-time grid intensity and selectively sourced from clean electricity. The battery-powered LRC offer better emission stability across regions due to their flexibility in charging strategies and lower exposure to local grid emissions during operation. From a systems perspective, meaningful emission reductions from vehicle electrification can be achieved only with the support of low-carbon electricity, and ongoing improvements in battery energy density, cost reductions, and the widespread deployment of charging infrastructure underpin its long-term viability and development trajectory. However, battery-electric trucks show greater consistency in performance across countries and may serve as a more robust transition pathway in areas where grid decarbonization is not yet complete. These findings reinforce the earlier conclusion that driving electrification, rather than refrigeration alone, holds the greatest mitigation potential for cold chain transport. However, realizing the full climate benefits of electrified refrigerated logistics will depend on overcoming barriers such as limited battery range, charging infrastructure gaps, and carbon-intensive grids. Targeted investments in battery innovation, smart routing, and clean power integration are therefore essential to accelerate this transition (Song et al., 2022; Telle et al., 2022; S. Zhang et al., 2023).

Alternative refrigerants are one of the emission reduction strategies in the refrigerated transportation sector. As shown in Fig. 6, although the proportion of refrigerant leakage in the entire life cycle of refrigerated transportation equipment is relatively small (8.26%—8.50%), its direct leakage into the atmosphere has a significant impact on the environment. In China, the commonly used refrigerants for refrigerated transportation equipment are R404A and R134A. Additionally, 5% of refrigerated transportation equipment still uses R22, which has a non-zero ODP and is in urgent need of being replaced. Meanwhile, refrigerants with medium to low GWP such as R134A and R744 have become alternative options. Thus, this study compares the impacts of replacing R404A with R744. Replacing R404A with R744 can reduce carbon emissions by 10.06% to 13.27%. It is worth noting that after the refrigeration unit uses R744, compared with R404A, both the COP and the refrigeration capacity have decreased, resulting in a 5.77% increase in carbon emissions related to refrigeration energy consumption. Therefore, when considering the replacement of refriger-

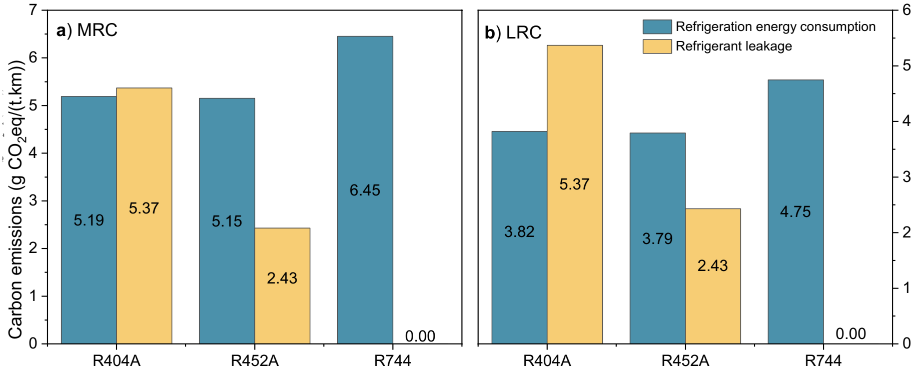

Fig. 6 Comparison of GHG emissions under different refrigerants

ants, it is not only necessary to take into account the ODP and GWP, but also the changes in refrigeration performance after the replacement, in order to comprehensively consider the actual effect after the replacement of refrigerants.

As shown in Fig. 7a, the life cycle carbon emissions of MRC show a significant reduction when transitioning from road to rail transport. Specifically, emissions decrease from 53.05 g CO_2eq/(t·km) under road transport to 19.65 g CO_2eq/(t·km) under rail transport—a reduction of 63.0%. Similarly, battery-powered LRC experience a decline from 51.94 to 18.54 g CO_2eq/(t·km), yielding a 64.3% reduction. These findings reinforce earlier studies (Li & Zhang, 2020; Tong et al., 2021), which report that road freight emits 7.9–10.5 times more CO_2 than rail freight per ton-kilometer. Given that road transport currently accounts for 89.73% of China's refrigerated logistics volume—while rail represents less than 1%—shifting even a fraction of long-distance freight to rail could result in substantial carbon savings. Previous estimates indicate that transferring 10% of road turnover to rail could cut emissions by over 22.5 million tons of CO_2 annually (Lin et al., 2017).

In addition to modal shift, logistics efficiency plays a key role in emissions reduction. Figure 7b evaluates the carbon emissions of MRC under varying empty load rates (i.e., the percentage of time vehicles operate without cargo). Reducing the empty load rate from 50 to

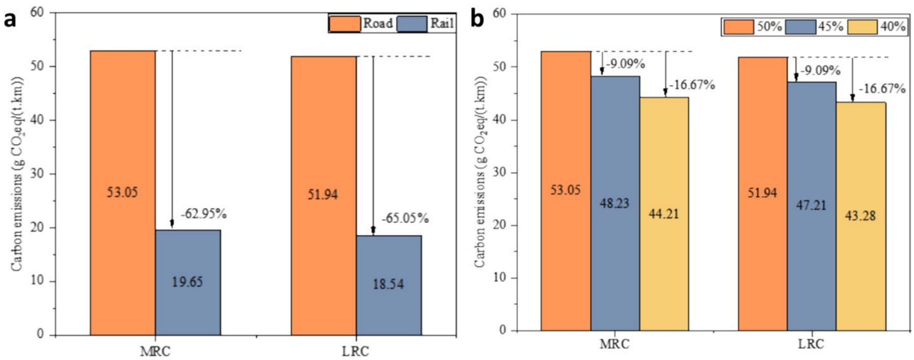

Fig. 7 Life cycle carbon emissions of LRC and MRC under different transport modes (**a**) and varying empty load rates (**b**)

40% leads to a decrease in emissions from 53.05 to 44.21 g CO_2eq/(t·km), which equates to a 16.67% reduction. The battery-powered LRC exhibits a similar improvement (from 51.94 to 43.28 g CO_2eq/(t·km), down 16.7%). This demonstrates the effectiveness of operational optimizations, such as route planning, vehicle matching algorithms, and dynamic scheduling, in reducing fuel use and improving load efficiency. Taken together, these findings underscore the dual importance of modal shift and transport optimization. Combining electrification strategies with rail substitution and smart logistics can offer substantial synergies in reducing the environmental footprint of cold chain freight systems.

3.4 Life cycle cost analysis

To comprehensively evaluate and support the application and promotion of the battery-based LRC, attention should not only be paid to its climate benefits but also to its economic feasibility throughout the entire life cycle. This study then conduct a life cycle cost analysis. Through quantitative analysis of the cost structure at different stages, this study aims to reveal the potential economic benefits of the LRC and provide a scientific and reliable quantitative basis for subsequent comprehensive decision-making. Owing to subsidy support, the purchase cost of the LRC is substantially reduced. When an LRC is acquired as a replacement following the scrappage of an MRC, the post-subsidy purchase price is approximately $25,000; by contrast, in the absence of MRC scrappage, the post-subsidy price of the LRC remains higher than that of the MRC, at around $40,000. However, this gap exhibits distinct stage-specific characteristics. With the continuous iteration of battery technology and the expansion of production scale, the cost of lithium batteries is expected to decline continuously in the next few years (Moreno Sader et al., 2025).

During the operation phase, both of these vehicles were powered by diesel engines. However, since the LFP equipped in LRC was heavier than the diesel engine in MRC, LRC required more fuel consumption to drive. For MRC, 675,376.43 L of diesel were needed, while LRC required 691,528.52 L of diesel. The cooling equipment of MRC directly relied on the electricity provided by diesel power generation to supply power, resulting in relatively high fuel consumption; the corresponding energy cost mainly depended on the fluctuations in diesel prices. In contrast, LRC utilized electricity to drive its cooling devices, achieving an optimized energy structure and reducing reliance on fossil fuels. According to the data in Table 3, the fuel consumption of MRC's cooling equipment was 71,064.64 L, and the corresponding fuel cost was $64,668.82. Under the same operating conditions, LRC powered by LFP batteries consumed 245,614 kWh of electricity. Even if calculated at a peak electricity price of $0.15 per kilowatt-hour, its electricity expenditure remained within $36,877.87. Compared to MRC, LRC could reduce energy costs by approximately 43% during the cooling phase, demonstrating significant operational economic advantages.

During the maintenance phases, the maintenance cost of the LRC system is slightly lower ($3,375 vs $5,100). As illustrated in Fig. 8, operation and maintenance costs constitute the dominant component of the life-cycle cost (LCC) for both vehicle systems, accounting for over 90% of the total LCC in each case. Upon the end of the refrigerated container's service life, the disposal cost is assumed to be 10% of the initial purchase cost, equals to approximately $4,500 for the LRC and $3,400 for the MRC. This portion of the cost primarily covers expenses associated with system disassembly, material recycling and treatment, and waste disposal. Through comprehensive calculation, the life-cycle cost of the LRC ranges

Table 3 The life-cycle cost analysis for the MRC and the LRC

The life-cycle cost of the MRC			
Acquisition cost ($)	34,000.00		
Total fuel consumption (L)	746,441.06		
Fuel cost ($/L)	0.91		
Total fuel cost ($)	679,261.37		
Maintenance cost ($)	5,100.00		
Disposal cost ($)	3,400.00		
Life-cycle cost ($)	721,761.37		
The life-cycle cost of the LRC			
Acquisition cost ($)	45,000.00		
Post-subsidy price ($)	25,000—40,000		
Total fuel consumption (L)	691,528.52		
Total fuel cost ($)	629,290.95		
Total electricity consumption (kWh)	245,614.04		
Electricity cost ($/kWh)	Off-peak	Basic	Peak
	0.04	0.09	0.15
Total electricity cost (kWh)	8,980.54	22,085.03	36,877.87
Maintenance cost ($)	3,375.00		
Disposal cost ($)	4,500.00		
Life-cycle cost ($)	667,646.49—691,146.49	680,750.98—704,250.98	695,543.82—719,043.82
Cost reduction (%)	5.06%–7.50%	3.24%–5.68%	1.19%–3.63%

from $581,200.54 to $609,097.87, which is lower than the MRC system's $623,138.82, representing an overall life-cycle cost reduction of 2.25% to 6.73%.

It is noteworthy that advancements in lithium-ion battery technology are manifested not only in cost reduction but also in enhanced energy density. Currently, the energy density of LFP batteries ranges from approximately 160 to 205 Wh/kg, and it is projected to exceed 300 Wh/kg in the coming years (Khan, 2026). An increase in energy density implies a reduction in the mass and volume of batteries required for the same energy storage capacity, thereby further cutting down costs in aspects such as system integration, transportation, installation, and maintenance. Higher energy density can also extend the operating duration, reduce fuel dependence, and indirectly lower fuel—related expenditures. Consequently, with the continuous upgrading of energy storage technology and dynamic shifts in the energy price structure, the economic performance of the LRC will exhibit a non—linear upward trend. Not only will the initial investment gradually decline, but the long—term energy—saving effects will also become more pronounced. In conclusion, while the LRC is currently constrained by lithium—ion battery costs, resulting in a slightly higher initial investment

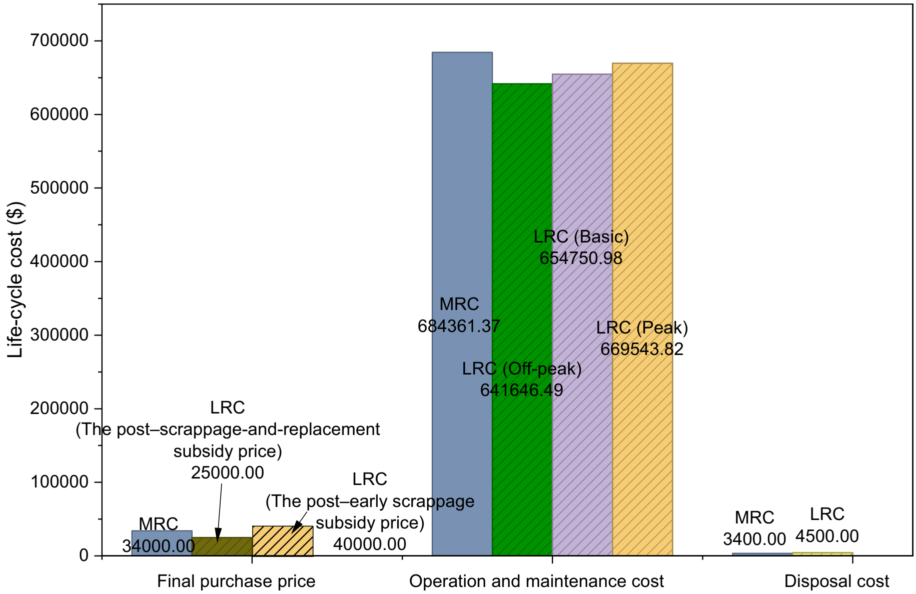

Fig. 8 The cost contribution of MRC and LRC at electricity prices of off-peak, basic, and peak respectively

compared to the traditional MRC, with the combined impact of decreasing battery unit prices and increasing energy density, its life-cycle economic efficiency is anticipated to significantly outperform that of the MRC. In the future, against the backdrop of mature energy storage technology and the transformation of the energy structure, the LRC will possess stronger cost competitiveness and extensive application and promotion value.

4 Conclusions

This study constructs cradle-to-grave LCA models for diesel-driven MRC and battery-based LRC to test whether electrified refrigeration yields net climate gains. In the base case, the battery-based LRC emits 2.10% less GHGs than MRC, a modest advantage explained by the dominance of the use phase, the small share of cooling within total traction-plus-cooling energy, the mass penalty of LRC (battery ~ 1.80 t; total 3.91 t) versus MRC (engine ~ 0.772 t; total 2.88 t), and the current carbon intensity of grid electricity. Moreover, LRC's manufacturing footprint is higher because of LFP production; battery recycling reduces this burden but yields only a limited lifecycle gain since production and end-of-life constitute a smaller share than operation. Additionally, sensitivity tests show that combining a 50% lower grid carbon intensity, best-available LFP manufacturing, and ~ 80% closed-loop recycling expands LRC's advantage by ~ 4–8 percentage points. Operational levers remain most influential: reducing empty-load from 50 to 40% lowers intensity by 16.67%, electrifying the traction side cuts ~ 14.14% (where grids are moderately clean), and deploying low-GWP refrigerants with tight leak control while maintaining COP delivers an additional ~ 1–3% lifecycle saving. When these supply- and demand-side measures are implemented together, the achievable lifecycle abatement reaches ~ 20–25% relative to today's MRC baseline. As battery technology advances and the energy structure optimizes, the life cycle cost advantage of the LRC will be further amplified, exhibiting enhanced economic competitiveness and scalability potential. Overall, electrification provides real but currently limited mitigation; maximizing benefits requires power-system decarbonization, lighter and cleaner battery supply chains with high-yield recycling, advancements in battery technology, and rigorous operational efficiency, while avoiding over-reliance on "electrify-only" narratives or refrigerant substitutions that compromise thermodynamic performance.

Building on the current focus on climate-related carbon footprint impacts, future research could be expanded to incorporate non-CO_2 effects and air pollutant impacts such as NO_x emissions and refrigerant-related ozone effects, which were beyond the scope of the present study. Moreover, moving beyond the diesel-vehicle assumptions adopted here, subsequent work may consider electrified transportation systems and more comprehensive, multi-dimensional environmental impact assessments to improve the robustness and generalizability of the findings. Additionally, future work should incorporate reliability and degradation dynamics (e.g., failure rates and performance decay) to assess how long-term system robustness may influence real-world environmental and economic outcomes.

Authors' contribution **Liu, G.,** : Conceptualization, data curation, validation, funding acquisition, writing – review. **Chen, Z.**: Methodology, model development, data analysis, writing – original draft. **He, Y.** **:** Data curation, writing – review. **Chang, H.**: Data curation, validation, writing – review. **Wu, J.**: Conceptualization, methodology, formal analysis, validation, supervision, writing – original draft.

Funding The author would like to thank the finance support from the Humanities and Social Science Fund of Ministry of Education of China, No.23YJA630060; Guangdong Office of Philosophy and Social Science, No.GD22CGL01; Guangzhou Municipal Science and Technology Program key projects, No.2024A03J0315.

References

Aliu, A., Imran, M. S., Dinh, T. Q., & Yoon, J. (2022). Thermal management of refrigeration unit for electric refrigerated vans: An experimental case study. *Energy Reports, 8*, 848–856. https://doi.org/10.1016/j.egyr.2022.10.269

Chinese association of refrigeration. (2025). *New trends in cold chain transportation equipment*. https://www.cr-expo.com/cn/xiangxi.aspx?id=825. Accessed 28 May 2025

Cui, Q., Gao, E., Huang, S., Chen, M., Yu, H., Zhang, Z., et al. (2025). Accounting and sensitivity analysis of CO2 emissions from typical food cold chain equipment in China. *Environmental Impact Assessment Review, 113*, 107881. https://doi.org/10.1016/J.EIAR.2025.107881

ISO 14044:2006. *Environmental management—Life cycle assessment—Requirements and guidelines*.International Organization for Standardization, Geneva, Switzerland. https://www.iso.org/standard/38498.html

Dong, Y., Coleman, M., & Miller, S. A. (2025). Greenhouse gas emissions from air conditioning and refrigeration service expansion in developing countries. *Annual Review of Environment and Resources, 44*, 5. https://doi.org/10.1146/annurev-environ-012220

Fabris, F., Fabrizio, M., Marinetti, S., Rossetti, A., & Minetto, S. (2024). Evaluation of the carbon footprint of HFC and natural refrigerant transport refrigeration units from a life-cycle perspective. *International Journal of Refrigeration, 159*, 17–27. https://doi.org/10.1016/J.IJREFRIG.2023.12.018

Farzaneh, F., & Jung, S. (2023). Lifecycle carbon footprint comparison between internal combustion engine versus electric transit vehicle: A case study in the U.S. *Journal of Cleaner Production*, 390, 136111. https://doi.org/10.1016/j.jclepro.2023.136111

Feng, R., Guo, W., Zhang, C., Nie, Y., & Li, J. (2025). Comparative study on environmental impact of electric vehicle batteries from a regional and energy perspective. *Batteries,*11, 23. https://doi.org/10.3390/batteries11010023

Feng, T., Guo, W., Li, Q., Meng, Z., & Liang, W. (2022). Life cycle assessment of lithium nickel cobalt manganese oxide batteries and lithium iron phosphate batteries for electric vehicles in China. *Journal of Energy Storage, 52*, 104767. https://doi.org/10.1016/J.EST.2022.104767

Guo, W., Feng, T., Li, W., Hua, L., Meng, Z., & Li, K. (2023a). Comparative life cycle assessment of sodium-ion and lithium iron phosphate batteries in the context of carbon neutrality. *Journal of Energy Storage, 72*, 108589. https://doi.org/10.1016/J.EST.2023.108589

Guo, X., Sun, Y., & Ren, D. (2023b). Life cycle carbon emission and cost-effectiveness analysis of electric vehicles in China. *Energy for Sustainable Development, 72*, 1–10. https://doi.org/10.1016/j.esd.2022.11.008

Han, D., Zhang, Y., Huang, C., Zheng, S., Wu, D., Li, Q., et al. (2024). Self-oscillating polymeric refrigerator with high energy efficiency. *Nature, 629*(8014), 1041–1046. https://doi.org/10.1038/s41586-024-07375-3

Hao, X., Zhou, D., Zhong, R., Li, S., Meng, X., & Liu, B. (2024). Electrification pathways for light-duty logistics vehicles based on perceived cost of ownership in Northern China. *Carbon Footprints*, *3*(3). https://doi.org/10.20517/cf.2024.24

He, Y.; Zhang, J.; Xu, W.; Wu, S.; Chang, H.; Yue, S.; Cao, Z. (2024). 40 Foot Lithium Battery Pure Electric Railway Development and Experimental Study of Refrigerated Container. *Journal of Refrigeration Technology*, *47*(2). https://doi.org/10.20094/j.issn.1674-0548.2024.02.035

Huo, D., Davies, B., Li, J., Alzaghrini, N., Sun, X., Meng, F., et al. (2024). How do we decarbonize one billion vehicles by 2050? Insights from a comparative life cycle assessment of electrifying light-duty vehicle fleets in the United States, China, and the United Kingdom. *Energy Policy, 195*, 114390. https://doi.org/10.1016/j.enpol.2024.114390

Huo, D., Davies, B., Li, J., Alzaghrini, N., Sun, X., Meng, F., et al. (2024b). How do we decarbonize one billion vehicles by 2050? Insights from a comparative life cycle assessment of electrifying light-duty vehicle fleets in the United States, China, and the United Kingdom, 195, 114390. *Energy Policy*. https://doi.org/10.1016/j.enpol.2024.114390

ISO 14067:2018. Greenhouse gases — Carbon footprint of products — Requirements and guidelines for quantification. International Organization for Standardization, Geneva, Switzerland: . https://www.iso.org/standard/71206.html

Jiang, R., Wu, C., Feng, W., You, K., Liu, J., Zhou, G., et al. (2025). Impact of electric vehicle battery recycling on reducing raw material demand and battery life-cycle carbon emissions in China, 15, 2267. *Scientific Reports*. https://doi.org/10.1038/s41598-025-86250-1

Kaptan, M., & Bayazit, O. (2023). Fuzzy Bayesian network analysis of the factors causing food losses in reefer containers, 46(7), e14358. *Journal of Food Process Engineering*. https://doi.org/10.1111/jfpe.14358

Khan, S. H. (2026). Energy storage systems for deep decarbonization: A critical review. *Journal of Energy Storage, 150*, 120485. https://doi.org/10.1016/J.EST.2026.120485

Li, A., Yu, B., Zhang, Y., Ouyang, H., Guo, Z., Shi, J., & Chen, J. (2024). The emission reduction potential and cost-effectiveness of low-GWP refrigerants in electric vehicle air conditionings. *Carbon Footprints*, *3*(2). https://doi.org/10.20517/cf.2023.54

Li, L., & Zhang, X. (2020). Integrated optimization of railway freight operation planning and pricing based on carbon emission reduction policies. *Journal of Cleaner Production, 263*, 121316. https://doi.org/10.1016/J.JCLEPRO.2020.121316

Lin, B., Liu, C., Wang, H., & Lin, R. (2017). Modeling the railway network design problem: A novel approach to considering carbon emissions reduction. *Transportation Research Part d: Transport and Environment, 56*, 95–109. https://doi.org/10.1016/j.trd.2017.07.008

Liu, G., Kuang, Z., Tang, J., Kuang, S., Tian, Q., Zou, Y., & Li, Q. (2024). Calculation and utility analysis of lychee life-cycle carbon emissions considering food loss and waste, 434, 140013. *Journal of Cleaner Production*. https://doi.org/10.1016/j.jclepro.2023.140013

Manjong, N. B., Usai, L., Orangi, S., Clos, D. P., & Strømman, A. H. (2024). Exploring raw material contributions to the greenhouse gas emissions of lithium-ion battery production. *Journal of Energy Storage, 100*, 113566. https://doi.org/10.1016/J.EST.2024.113566

Moreno Sader, K., Biswas, S., Jones, R., Mennig, M., Rezaei, R., & Green, W. H. (2025). Battery electric long-haul trucking with overnight charging in the United States: A comprehensive costing and emissions analysis. *Applied Energy, 384*, 125443. https://doi.org/10.1016/J.APENERGY.2025.125443

Qiao, Q., Zhao, F., Liu, Z., Hao, H., He, X., Przesmitzki, S. V., & Amer, A. A. (2020). Life cycle cost and GHG emission benefits of electric vehicles in China. *Transportation Research Part d: Transport and Environment, 86*(1), 102418. https://doi.org/10.1016/j.trd.2020.102418

Quan, Y., Cao, G., & Zhang, Q. (2025). Assessing the environmental benefits and carbon emission reduction potential of lithium-ion batteries and internal combustion engines for vehicles. *Journal of Environmental Sciences*.Available online 13 December 2025. https://doi.org/10.1016/J.JES.2025.12.007

Ritchie et. al. (2020). Electricity Mix. *Our World in Data*. https://ourworldindata.org/electricity-mix. Accessed 11 June 2025

Song, H., Cai, M., Cen, J., Xu, C., & Zeng, Q. (2022). Research on energy saving optimization method of electric refrigerated truck based on genetic algorithm. *International Journal of Refrigeration, 137*, 62–69. https://doi.org/10.1016/j.ijrefrig.2022.02.003

Tao, Y., Sun, T., & Wang, Z. (2023). Uncovering various paths for environmentally recycling lithium iron phosphate batteries through life cycle assessment. *Journal of Cleaner Production, 393*, 136263. https://doi.org/10.1016/J.JCLEPRO.2023.136263

Telle, J. S., Schlüters, S., Schönfeldt, P., Hanke, B., von Maydell, K., & Agert, C. (2022). The optimized integration of temperature-controlled transports into distributed sector-integrated energy systems, 269, 116148. *Energy Conversion and Management*. https://doi.org/10.1016/j.enconman.2022.116148

Tong, H., Peng, J., Zhang, Y., Fang, T., Zhang, J., Men, Z., et al. (2021). Environmental benefit analysis of "road-to-rail" policy in China based on a railway tunnel measurement. *Journal of Cleaner Production, 316*, 128227. https://doi.org/10.1016/J.JCLEPRO.2021.128227

Wan, T., Fu, H., Li, X., Wu, F., Luo, C., & Zhang, L. (2025). Assessment of decarbonization pathway for Chinese road transport sector based on transportation-energy integration systems framework, 317, 134727. *Energy* . https://doi.org/10.1016/j.energy.2025.134727

Wang, Y., Shan, X., & Qiu, R. (2025). Lifecycle carbon dioxide emissions and cost assessment for battery electric bus systems. *Journal of Cleaner Production, 501*, 145278. https://doi.org/10.1016/J.JCLEPRO.2025.145278

Volvo Cars. (2023).Climate action. Volvo Cars China. (accessed February 2026). https://www.volvocars.com.cn/zh-cn/sustainability/climate-action/

Wu, J., Li, Q., Liu, G., Xie, R., Zou, Y., Scipioni, A., & Manzardo, A. (2022). Evaluating the impact of refrigerated transport trucks in China on climate change from the life cycle perspective, 97, 106866. *Environmental Impact Assessment Review*. https://doi.org/10.1016/j.eiar.2022.106866

Wu, J., Liu, G., Marson, A., Fedele, A., Scipioni, A., & Manzardo, A. (2022). Mitigating environmental burden of the refrigerated transportation sector: Carbon footprint comparisons of commonly used refrigeration systems and alternative cold storage systems, 372, 133514. *Journal of Cleaner Production*. https://doi.org/10.1016/j.jclepro.2022.133514

Zhang, L., Wei, J., & Tu, R. (2024a). Temporal-spatial analysis of transportation CO2 emissions in China: Clustering and policy recommendations. *Heliyon, 10*(2), e24648. https://doi.org/10.1016/J.HELIYON.2024.E24648

Zhang, S., Guan, C., Qiu, Y., & Wu, N. (2023). Multi-objective route optimization of urban cold chain distribution using electric and diesel powered vehicles, 49, 100969. *Research in Transportation Business and Management*. https://doi.org/10.1016/j.rtbm.2023.100969

Zhang, W., Li, Y., Li, H., Liu, S., Zhang, J., & Kong, Y. (2024b). Systematic review of life cycle assessments on carbon emissions in the transportation system, 109, 107618. Environmental Impact Assessment Review https://doi.org/10.1016/j.eiar.2024.107618

Zhang, X., Bai, X., Ma, F., & Wang, Y. (2025). Economic and environmental feasibility assessment of emerging biometallurgical recycling methods for spent electric-vehicle batteries, 40, 104369 . *Environmental Technology and Innovation*. https://doi.org/10.1016/j.eti.2025.104369

Authors and Affiliations

Guanghai Liu[1] · Zongyu Chen[1] · Yuanxin He[2] · Hai Chang[2] · Junzhang Wu[3]

✉ Junzhang Wu
junzhang.wu@unipd.it

Guanghai Liu
broadsea@gzhu.edu.cn

Zongyu Chen
mounianu@e.gzhu.edu.cn

Yuanxin He
wujunz2020@gmail.com

Hai Chang
2664599311@qq.com

1 Research Centre for Cold Chain and Standardization, School of Management, Guangzhou University, Guangzhou 510006, China

2 CRRC Yangtze Co., Ltd., Daqiao New Area, Jiangxia Economic Development Zone, Wuhan 430212, China

3 Department of Civil, Environmental and Architectural Engineering, University of Padova, Via Marzolo 9, 35131 Padua, Italy